

II-B Laser Cooling and Trapping of Metastable Helium Atoms

In the past two decades, extensive developments have occurred in the laser cooling and trapping of neutral atoms, with many workers reporting the application of these techniques to such diverse atomic species as alkali atoms, alkali earth atoms, and rare gas atoms. Among these, the helium atom is unique on account of its small mass, simple energy level structure, and easy availability in two isotopic forms (^3He and ^4He) of differing quantum statistics. For this reason, we have been studying the laser cooling and trapping of helium atoms.

II-B-1 Magneto-Optical Trap of Metastable Helium Atoms with Doughnut Laser Beams: Computer Simulations

MORITA, Norio

When we intend to confine metastable helium atoms in high density in a magneto-optical trap (MOT), it is always a critical problem that the collisional ionization loss of the atoms is tremendously large under the irradiation of trapping laser light near-resonant with the cooling transition ($2s^3S_1 \rightarrow 2p^3P_2$). One of the possible methods that can let us avoid this problem may be to use laser beams with doughnut intensity profiles, because a MOT composed of such laser beams has almost negligible laser intensity around the MOT center. However, such a MOT has never been investigated so far and it is not trivial whether this type of MOT can efficiently confine the atoms. Therefore, with a computer simulation we have examined the availability of this MOT. First let us consider a one-dimensional MOT composed of doughnut laser beams: in this case, an atom lying at the center of the beam cross section and moving parallel to the beam axis receives no force

from the beam, and so this atom can be neither decelerated nor trapped by the beam. This means that it is necessary to stop up the "hole" of the MOT by, for example, additional laser beams. Taking this into consideration, we can find that the simplest and most symmetric three-dimensional MOT that has no such "holes" may be a MOT with a dodecahedral beam configuration, which consists of eight doughnut beams coming from apexes of a dodecahedron to its center. Note that this configuration can easily be realized by a simple modification of a usual tetrahedral configuration. We have numerically simulated the atomic motion in this type of MOT, which is composed of eight laser beams with ($n = 0, l = 1$) Laguerre-Gaussian intensity profiles (the peak intensity is 20 mW/cm^2 and the radius of the peak ring is 3 mm). Consequently, we have found that any atom can be confined within a radius of 0.1 mm, in which only $< 0.5\%$ of the atoms are excited into the upper state of the cooling transition by the lasers. This means that the atomic density in the MOT can be increased by a factor of more than five in comparison with an ordinary MOT in the full saturation condition. An experiment to prove this result is now in progress.

II-C Spectroscopic Studies on Atoms and Ions in Liquid Helium

Atoms and ions in liquid helium are known to reside in bubble-like cavities due to the Pauli repulsive force between electrons. Physical properties of these exotic surroundings are determined by the potential energy of the impurity- He_n system, the surface tension energy of the liquid helium, and the pressure-volume work. Spectroscopic studies of such impurity atoms and ions in liquid helium are expected not only to give information on the structure and dynamics of the bubbles but also to contribute to the study on the property of superfluid liquid helium.

II-C-1 Investigation on the Difference between Spectra of Ca Atoms in Liquid ^3He and ^4He

MORIWAKI, Yoshiki¹; MORITA, Norio
(¹Toyama Univ.)

Spectra of impurity atoms in liquid helium often explicitly reflect physical properties of the liquid. In this meaning, it may especially be interesting to investigate the difference between spectra of impurity atoms in liquid ^3He and ^4He , because even at a temperature as high as 1.4 K these liquids have much different physical properties; for example, the density is 1.62×10^{22} and $2.19 \times 10^{22} \text{ cm}^{-3}$ for ^3He and ^4He , respectively, and the

surface tension is 0.116 and 0.336 dyn/cm for ^3He and ^4He , respectively. These differing properties are mainly caused by differences in the mass and quantum statistics between each species of He. In this work we have experimentally obtained spectra of Ca atoms in liquid ^3He and ^4He at 1.4 K and have investigated their differences. The experimental excitation spectra of the $4s^2 \ ^1S_0 \rightarrow 4s4p \ ^1P_1$ and $4s4p \ ^3P_{0,1,2} \rightarrow 4s5s \ ^3S_1$ transitions are shown in Figures 1 (a) and (b), respectively. For each transition, as seen in these figures, the spectrum for liquid ^3He is narrow compared with the one for liquid ^4He , and the blue-shift of the former spectrum is smaller than the latter. This fact can qualitatively be explained with differences in the

number density and surface tension of the liquid; namely, in liquid ^3He , the size of a bubble formed around an impurity Ca atom is larger because of the smaller number density and surface tension of liquid ^3He , and this causes the Ca-He interaction the weaker. To confirm this, we have theoretically calculated these spectra, assuming a model Hamiltonian describing the Ca atom, bubble and their interactions for each liquid He. This Hamiltonian has almost the same form as assumed in our previous work on Yb^+ in liquid He. The spectra thus calculated are shown in Figures 1 (c) and (d), corresponding to Figures 1 (a) and (b), respectively. Comparing Figures 1 (a) and (b) with Figures 1 (c) and (d), respectively, we can see that the calculated results considerably well reproduce both widths and shifts of the experimental spectra. This fact strongly suggests that the differences observed in the experimental spectra are mainly caused by the differences in the physical properties of liquid ^3He and ^4He .

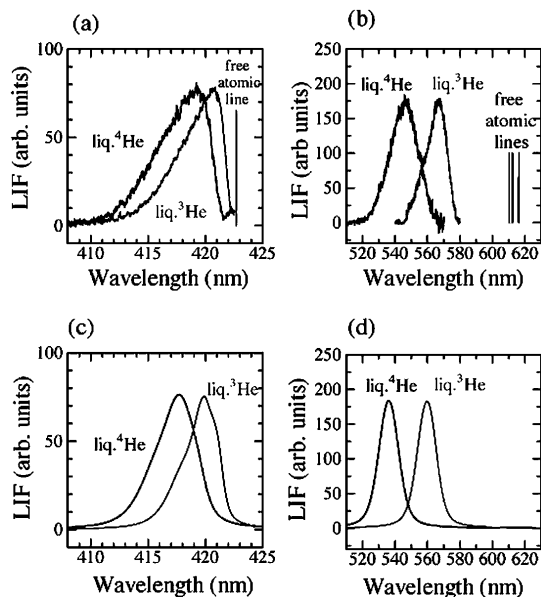


Figure 1. Excitation spectra of Ca atoms in liquid ^3He (gray curves) and ^4He (black curves): (a) and (b) show the experimental spectra of the $4s^2\ ^1S_0 \rightarrow 4s4p\ ^1P_1$ and $4s4p\ ^3P_{0,1,2} \rightarrow 4s5s\ ^3S_1$ transitions, respectively, and the theoretical spectra of those transitions are shown in (c) and (d), respectively. In (a) and (b), each transition wavelength of the free atom is also shown with a solid vertical line.

II-D Laser Spectroscopic Studies on Collisional Fine Structure Changing Transitions of Atoms and Ions

The fine structure changing transition in atoms and ions due to collisions with other particles is one of the important processes for the energy transportation in interstellar gases as well as in the atmosphere. However, unexpectedly, the number of studies so far devoted to the measurement of the cross section for this process is not so large. For this reason, we have been studying this process with laser spectroscopic methods, mainly focusing on alkali-earth ions, which have simpler energy level structures and so allow us to analyze experimental results more easily.

II-D-1 Laser Spectroscopic Measurements of Fine Structure Changing Cross Sections of Ba^+ Ions in Collisions with He Atoms

MORIWAKI, Yoshiki¹; MATSUO, Yukari²;
MORITA, Norio
(¹Toyama Univ.; ²RIKEN)

We have measured the cross section of the fine structure changing $6p\ ^2P_{3/2} \rightarrow 6p\ ^2P_{1/2}$ transition of the Ba^+ ion in collisions with He atoms at a room temperature. Like our similar work on Ca^+ and Sr^+ , Ba^+ ions have been produced by laser ablation of a piece of BaTiO_3 placed in a vacuum chamber. The chamber is filled with He gas, and the ions produced are immediately cooled to a room temperature through collisions with the He atoms. Exciting the ions into the $6p\ ^2P_{3/2}$ level and detecting the laser-induced fluorescence from $6p\ ^2P_{3/2}$ and the sensitized

fluorescence from $6p\ ^2P_{1/2}$ we have successfully obtained cross sections of the collision-induced $6p\ ^2P_{3/2} \rightarrow 6p\ ^2P_{1/2}$ transition and of the collisional quenching in the $6p\ ^2P_{1/2}$ level: $\sigma(6p\ ^2P_{3/2} \rightarrow 6p\ ^2P_{1/2}) = (2.9 \pm 0.4) \times 10^{-4}\ \text{\AA}^2$ and $\sigma(6p\ ^2P_{1/2} \rightarrow \text{all states}) = (4.2 \pm 7.9) \times 10^{-2}\ \text{\AA}^2$. Figure 1 shows the cross sections for the $np\ ^2P_{3/2} \rightarrow np\ ^2P_{1/2}$ transitions of various alkali metal atoms as well as alkali earth ions in the logarithmic scale as a function of their fine structure splittings. As seen in Figure 1, the cross sections for the alkali atoms are almost on a straight line; those for the alkali earth ions are also roughly on a straight line, but its slope is much different from the one for the alkali atoms. These exponential decreases common to both the ions and atoms can be explained by the Landau-Zener theory, as described in the previous work. On the other hand, the differing slopes of the decreases may be due to a difference between the interactions for ion-He and atom-He pairs; namely, the interaction in an ion-He pair is mainly the

monopole-induced-dipole interaction, which is stronger than for an atom-He pair. This fact may result in that, assuming the same fine structure splitting, the cross section for an alkali earth ion is much larger than for an alkali atom, as seen in Figure 1.

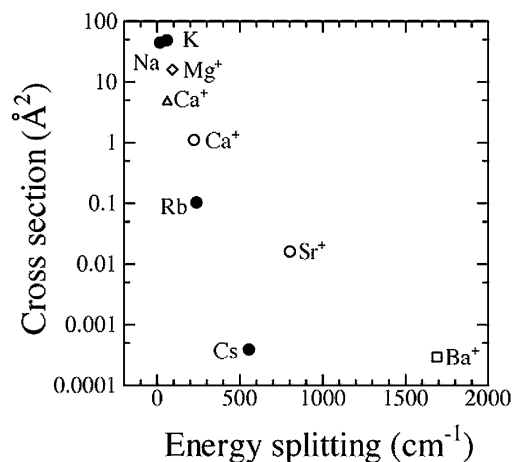


Figure 1. Fine structure changing cross sections so far measured for various alkali atoms and alkali earth ions in collisions with He atoms, as a function of their fine structure splittings; ● shows the one for the $np\ ^2P_{3/2} \rightarrow np\ ^2P_{1/2}$ transition of each alkali atom ($n = 3, 4, 5$ and 6 , and the collision temperature $T = 397, 368, 340$ and 311 K for Na, K, Rb and Cs, respectively) (by Krause), ◇ $Mg^+ 3p\ ^2P_{3/2} \rightarrow 3p\ ^2P_{1/2}$ at 1600 K (by Brust *et al.*), △ $Ca^+ 3d\ ^2D_{5/2} \rightarrow 3d\ ^2D_{3/2}$ at 10000 K (by Knoop *et al.*), ○ $Ca^+ 4p\ ^2P_{3/2} \rightarrow 4p\ ^2P_{1/2}$ and $Sr^+ 5p\ ^2P_{3/2} \rightarrow 5p\ ^2P_{1/2}$ at 298 K (by Moriwaki *et al.*) and □ the present data.

II-D-2 Measurements of Fine Structure Changing Cross Sections of Ca^+ , Sr^+ and Ba^+ Ions due to Collisions with H_2 and D_2 Molecules

MORIWAKI, Yoshiki¹; MATSUO, Yukari²;
MORITA, Norio
(¹Toyama Univ.; ²RIKEN)

Because of the vibrational and rotational degrees of freedom in molecules, fine structure changing transitions of ions due to collisions with molecules may show unique properties different from the ones in collisions with spherical atoms like He. For this reason, we have measured cross sections for such transitions of Ca^+ , Sr^+ and Ba^+ ions in collisions with H_2 and D_2 molecules. The experimental procedure is almost the same as in the previous ion-He collision studies, except for filling the vacuum chamber with H_2 or D_2 gas instead of He. The cross sections obtained are summarized in Table 1. For the $np\ ^2P_{3/2} \rightarrow np\ ^2P_{1/2}$ transitions, as seen in Table 1, there are no drastic differences in the cross sections among each ion. This is completely different from the behavior seen in collisions with He. On the other hand, it is quite interesting that the ratio between the cross sections for the collisions with H_2 and D_2 decreases with the increase of the fine structure splitting, which is $222, 802$ and $1690\ cm^{-1}$ for Ca^+ , Sr^+ and Ba^+ , respectively. Considering this fact as well as the sizes of the splittings, we can find that not vibrational transitions but

rotational transitions of the molecules resonantly contribute to the collisional fine structure changing transitions of the ions. To confirm this, we have theoretically calculated the cross section ratios, based on a semi-classical theory (Anderson-Tsao-Curnutte theory) taking into consideration the degree of resonance between fine structure splittings of the ions and rotational transitions of the molecules. As seen in Table 1, the experimental ratios are well reproduced by our theoretical calculation.

Table 1. Fine structure changing cross sections of Ca^+ , Sr^+ and Ba^+ due to collisions with H_2 and D_2 .

Ion	Transition	Cross Sections (\AA^2)		$\sigma(D_2)/\sigma(H_2)$	
		$\sigma(H_2)$	$\sigma(D_2)$	exp.	calc.
Ca^+	$4p\ ^2P_{3/2} \rightarrow 4p\ ^2P_{1/2}$	13.2 ± 0.6	18.7 ± 0.8	1.4	1.6
Ca^+	$4p\ ^2P_{1/2} \rightarrow 4p\ ^2P_{3/2}$	20.5 ± 0.9	27.1 ± 1.3	1.3	
Sr^+	$5p\ ^2P_{3/2} \rightarrow 5p\ ^2P_{1/2}$	22.7 ± 0.4	18.0 ± 0.4	0.82	0.7
Ba^+	$6p\ ^2P_{3/2} \rightarrow 6p\ ^2P_{1/2}$	11.5 ± 0.1	3.9 ± 0.2	0.33	0.3